Fission and Deep Spallation Characteristics in Relativistic Nuclear Collisions

A. I. Warwick, A. Baden,[a] H. H. Gutbrod, M. R. Maier, J. Péter,[b] H. G. Ritter, H. Stelzer, H. H. Wieman, and F. Weik

Gesellschaft für Schwerionenforschung, Darmstadt 0-6100, West Germany, and Nuclear Science Division, Lawrence Berkeley Laboratory, University of California, Berkeley, California 94720

and

M. Freedman, D. J. Henderson, S. B. Kaufman, E. P. Steinberg, and B. D. Wilkins

Argonne National Laboratory, Argonne, Illinois 60439

(Received 12 March 1982)

Numbers of emitted fast charged particles associated with heavier nuclear fragments are employed as a graphic means of differentiating fission and spallation contributions to target fragment emission in relativistic nuclear collisions. The violent nature of the deep spallation mechanism is observed directly.

PACS numbers: 25.70.Bc, 25.70.Fg

Radiochemists have studied the breakup of nuclear targets bombarded with high-energy projectiles (usually protons) for many years.[1-7] More than one reaction mechanism has been perceived to contribute to the production of fragments of intermediate mass. For example, in the bombardment of U with protons at incident kinetic energies up to 2 GeV, neutron-excess fragments of mass approximately half that of the target exhibit typical fission-product kinetic energy spectra[1,2] (derived from differential range measurements). This has been interpreted as an indication of their origin in nonviolent collisions. Neutron-deficient products in this mass range, however, exhibit much lower kinetic energies and are said to arise from a deep spallation mechanism,[1-3] which is not well understood.

The deep spallation mechanism produces fragments across a broad mass range and can be studied as a function of fragment mass. Other features of interest are the momentum transferred to the nuclear system, its excitation energy, its initial mass, and the associated emission of fast light particles. Multidetector measurements of nuclear collisions, analyzed event by event, provide a means of studying the interdependence of all these observables. However, the yield of fragments of intermediate mass contains a contribution from fission. This has been observed from high-energy collisions on targets as light as silver.[8] It is therefore important to be able to distinguish fission from deep spallation on an event-by-event basis.

Radiochemical techniques are not appropriate to the study of the interdependence of several observables. Detector experiments measuring the neutron-to-proton ratio of the fragments could, in principle, separate fission events from spallation but the simultaneous measurement of fragment mass and charge to the required accuracy is beyond the reach of present experimental techniques.

In this article we present the first results of a detailed multidetector experiment and achieve a rather clear separation between fission and spallation events both by detecting the fission partners in a large-area detector and by counting the number of fast charged particles emitted from the collisions. The latter technique is novel and more illuminating, since the number of emitted fast particles is also a measure of the violence of the initial stage of the collision. We confine ourselves here to results for a range of fragment mass ($80 \leq A \leq 89$) where there is a large contribution from fission, and we examine the characteristics of the collisions for several different projectiles (4.9-GeV protons, 250-MeV/u neon, and 2.1-GeV/u neon).

That part of the experimental arrangement that is relevant to this report consisted of a time-of-flight arm at $\theta \simeq 90°$ in the laboratory frame for the detection of the heavy fragments. This was made up of a large-area, thin (150 μg cm^{-2}) avalanche detector as the start counter, and several silicon surface-barrier detectors as the stop and energy-measuring detectors. The target was also thin (500 μg cm^{-2}) and mounted at an oblique angle, 15° to the beam, giving sensitivity to the slow heavy fragments emerging at $\theta = 90°$, provided their kinetic energy was greater than a threshold of about 0.2 MeV per mass unit. A second similar avalanche counter at $\theta \simeq 90°$ on the opposite side of the beam allowed the selection of data for binary or nonbinary breakup of the target residue. Studies of binary breakup kinematics[4] show that before breakup the residue

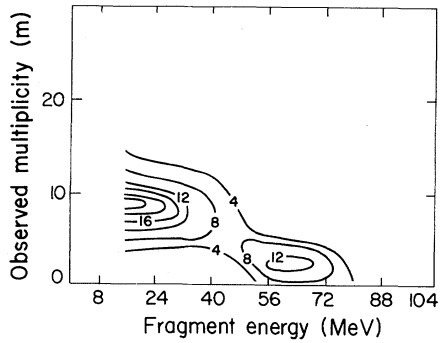

FIG. 1. Contours of fragment yield (arbitrary units) in the mass range $80 \leq A \leq 89$ at $\theta = 90°$ from the bombardment of ^{197}Au by ^{20}Ne projectiles at 250 MeV/u.

moves slowly ($\beta \lesssim 0.003$) such that the 180° correlation in the center-of-mass frame is approximately preserved in the laboratory frame. Surrounding the thin-walled spherical scattering chamber, an array of 80 scintillators measured the number of fast charged particles[4] associated with the fragment emission, providing a direct measurement of the degree of violence of each collision.

We are concerned here with the gross features of the reaction, those mechanisms with enough cross section to contribute significantly to the singles yield of the fragments. Thus, for example, mechanisms such as ternary fission are not discussed.

Figure 1 (for 250-MeV/u Ne + Au) shows the singles yield of fragments as a contour plot versus the fragment kinetic energy and the observed associated multiplicity of fast charged particles detected in the 80-fold scintillator array. (Observed multiplicity means simply the number of scintillators hit by a fast charged particle in coincidence with the fragment; no correction for double hits or missing solid angle is made in this report.) There are clearly two components to the yield, corresponding to two different reaction mechanisms responsible for the major yield of fragments in this mass range. The high-multiplicity component (from more violent collisions) has low kinetic energy and the very low-multiplicity component (from very gentle collisions) exhibits a fissionlike energy spectrum, peaking at 60-65 MeV.

There is some overlap of the mechanisms when the yield is plotted as in Fig. 1, but we can separate the two components in the following way. The energy spectrum at high multiplicity ($m > 10$) is taken as the shape of the low-energy, high-multiplicity component and renormalized to the total yield at the lowest fragment energies (15–20

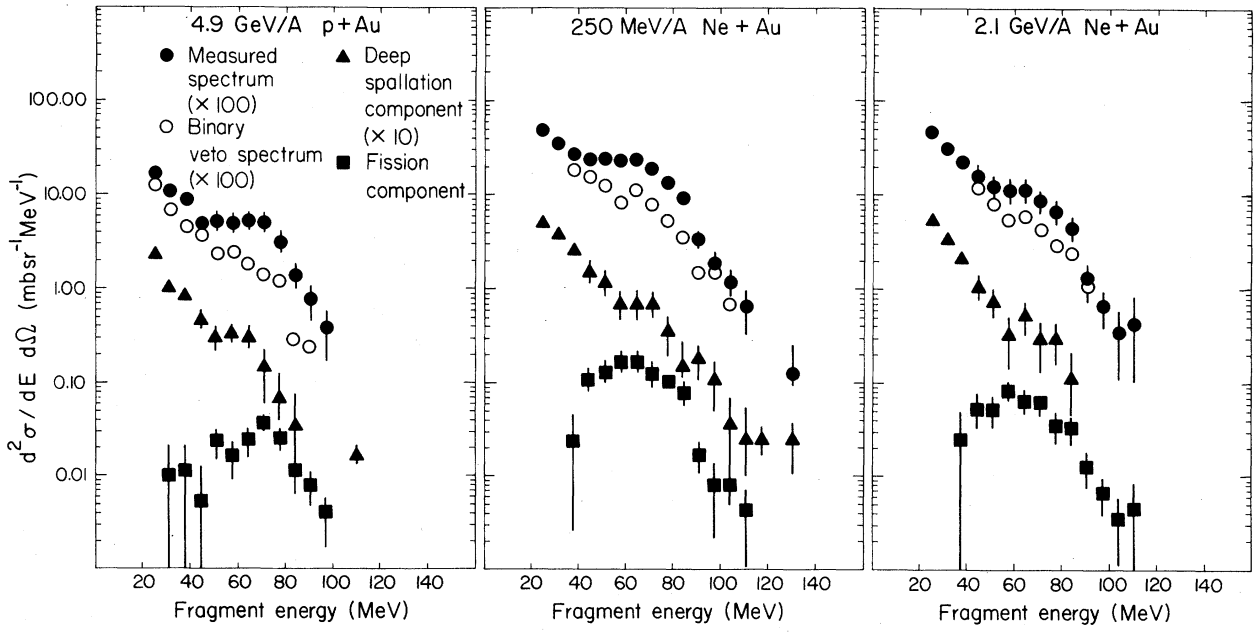

FIG. 2. Energy spectra of fragments in the mass range $80 \leq A \leq 89$ at $\theta = 90°$ from three different bombardments. The upper curves (solid circles) are the measured yield; the open circles are from nonbinary events (see text). The lower curves are the results of the multiplicity separation into the fission and deep-spallation components (see text).

MeV) where it is the only contribution. (Studies of the multiplicity associated with heavier fragments, where the fission component is small, show that the kinetic energy distribution of these fragments is approximately independent of the multiplicity.) The renormalized result is the spectrum of the low-energy component; the remaining yield is the energy spectrum of the high-energy, low-multiplicity component.

Figure 2 shows the results of such a procedure for several reactions. The absolute normalization of the data is uncertain by 30% for the 4.9-GeV/u proton and 2.1-GeV/u Ne cases, somewhat more uncertain for the case of 250-MeV/u Ne. The high-multiplicity component (solid triangles) shows an exponential energy spectrum; the low-multiplicity spectrum (solid squares) peaks around 60 MeV.

We now demonstrate explicitly the binary nature of the low-multiplicity component by employing the second thin avalanche detector on the opposite side of the beam to the measured fragment to count the heavy partner from the binary breakup. The geometry of the detectors is such that binary events are counted if the difference in the θ angles of the two fragments lies approximately between 150° and 210° in the laboratory frame. A similar analysis has been presented by Meyer *et al.*[9] using data from the forerunner to this experiment. The avalanche counters (with an appropriate software threshold) are not sensitive to alpha particles; their efficiency climbs to 100% for fragments of mass $A \simeq 15$ in the energy range of interest; however, the software threshold is set at about $A = 30$. Figure 3, for 250-MeV/u Ne + Au, shows the observed multiplicity distribution associated with the fragments (a) without a heavy partner firing the opposite avalanche detector (binary veto); (b) with a heavy partner (binary). Clearly the low-multiplicity component is binary and the high-multiplicity component is not.

Also shown, as open circles in Fig. 2, are the energy spectra of events satisfying the binary veto requirement. These spectra are essentially the same as the high-multiplicity component from the separation procedure outlined above.

The high-multiplicity component of the heavy-fragment yield observed here comes from a reaction mechanism that has been loosely termed "deep spallation" in previous studies. This is a violent process. The residual fragments have exponentially falling energy spectra (Fig. 2) with a slope parameter $\tau \simeq 15$ MeV. For heavier fragments ($120 \leq A \leq 139$), where there is much less

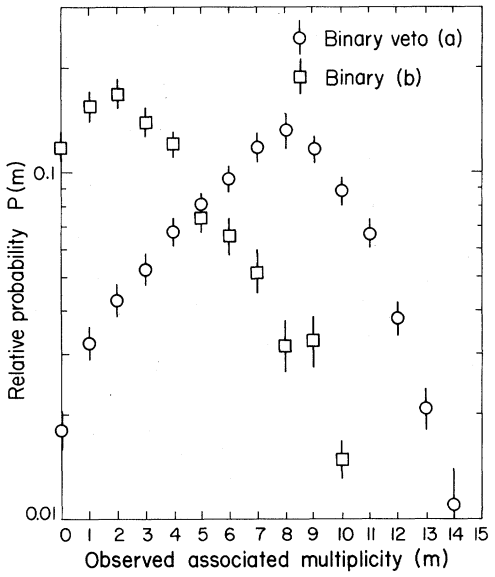

FIG. 3. Observed fast-charged-particle multiplicity distributions associated with fragments from binary and nonbinary breakup. The fragments are in the mass range $80 \leq A \leq 89$ at $\theta = 90°$ from the reaction 250-MeV/u Ne + Au.

contribution from fission, the slope is steeper ($\tau \simeq 8$ MeV). The low-multiplicity reaction mechanism is binary fission. The mean fast-particle observed multiplicity associated with fission shows little energy dependence, changing from $\langle m \rangle = 2$ at 250 MeV/u to $\langle m \rangle = 3$ for 2.1 GeV/u Ne + Au. The mean observed multiplicity associated with spallation, however, increases from $\langle m \rangle = 8$ at 250 MeV/u to $\langle m \rangle = 15$ for 2.1 GeV/u Ne + Au.

In conclusion, we have graphically differentiated between the reaction mechanisms of fission and deep spallation by employing multiplicity measurements to observe directly the violence of the collisions associated with these two processes. We can separate the mechanisms both by the multiplicity technique and by observing the binary or nonbinary nature of the final state and obtain the same spectral components by both methods. We have thus measured energy spectra of deep spallation fragments and we have opened the way for more detailed studies of the features of this mechanism as a function of fragment mass from the lighter fragments, through the fission region, to the heaviest fragments produced.

We acknowledge the support and encouragement of A. M. Poskanzer. This work was supported in part by the Director, Office of Energy Research, Division of Nuclear Physics of the Office of High

Energy and Nuclear Physics of the U. S. Department of Energy, under Contracts No. DE-AC03-76SF00098 and No. W31-109-ENG-38.

[a]Present address: Department of Physics, University of California, Berkeley, Cal. 94720.
[b]Present address: Institut de Physique Nucléaire, F-91406 Orsay, France.

[1]V. P. Crespo, J. B. Cumming, and A. M. Poskanzer, Phys. Rev. 174, 1455 (1968).
[2]N. T. Porile, S. Pandian, H. Klonk, C. R. Rudy, and E. P. Steinberg, Phys. Rev. C 19, 1832 (1979), and references therein.
[3]V. P. Crespo, J. B. Cumming, and J. M. Alexander, Phys. Rev. C 2, 1777 (1970).
[4]G. Friedlander, *Physics and Chemistry of Fission* (International Atomic Energy Agency, Vienna, 1965), Vol. II, p. 265.
[5]R. Brandt, *Physics and Chemistry of Fission* (International Atomic Energy Agency, Vienna, 1965), Vol. II, p. 329.
[6]L. P. Remsberg, F. Plasil, J. B. Cumming, and M. L. Perlman, Phys. Rev. 187, 1597 (1969).
[7]S. B. Kaufman, E. P. Steinberg, B. D. Wilkins, and D. J. Henderson, Phys. Rev. C 22, 1897 (1980).
[8]R. Brandt, F. Carbonara, E. Cieslak, H. Piekarz, J. Piekarz, and J. Zakrzewski, Rev. Phys. Appl. 7, 243 (1972).
[9]W. G. Meyer, H. H. Gutbrod, C. Lukner, and A. Sandoval, Phys. Rev. C 22, 179 (1980).

Atomic Cascade of Muonic and Pionic Helium Atoms

R. Landua and E. Klempt
Institut für Physik, Universität Mainz, D-6500 Mainz, Germany
(Received 15 December 1980; revised manuscript received 22 February 1982)

The cascade of muonic and pionic helium atoms in targets of arbitrary density is investigated. The calculation does not use any free parameters except for strong-interaction effects. All measured x-ray intensities are reproduced, in particular the K_β/K_α intensity ratios in pionic helium.

PACS numbers: 36.10.-k, 32.30.Rj

Energies and intensities of x rays emitted in the cascade of muonic and pionic helium atoms were determined in several experiments[1-5] but as yet there appears to be no adequate quantitative understanding of the cascade process. In contrast to heavy exotic atoms the exotic helium ion $(\text{He-}M)^+$ has no electron cloud of its own and therefore experiences, in collisions with neighboring helium atoms, strong and fluctuating electric fields and electron densities inducing Stark and Auger transitions, respectively.[6] The situation is also different from that of the mesonic hydrogen problem,[7,8] where the exotic atom forms a neutral system. Earlier cascade calculations on exotic helium atoms[3,9] were based on a phenomenological picture using free parameters for Stark mixing and Auger rates, which were separately determined for each system and for different densities. The purpose of this Letter is to describe a calculation of the cascade of exotic helium atoms *without any free parameter* for these effects.

The atomic cascade in helium starts after the capture of the free negative particle M with mass m which proceeds generally via the Auger effect. Then the meson is bound in an atomic orbit around the alpha particle. It is assumed that it is captured into orbits with principal quantum numbers $n_c = (m_M/m_e)^{1/2}$; n_c is about 14 for muons and 16 for pions. The second electron is ejected during the first deexcitation step via the internal Auger effect unless Auger transitions are suppressed in almost circular atomic states. Recombination of the protonlike ion $(\text{He-}M)^+$ with electrons of colliding helium atoms is prohibited because of energy conservation.

Deexcitation of the $(\text{He-}M)^+$ ion can occur by radiation or by the external Auger effect. For high n and for experimentally accessible helium densities the deexcitation proceeds exclusively via the external Auger effect with a rate increasing linearly with density. For levels below $n = 4$–7, depending on the system and the density, the rate for radiative transitions becomes comparable to or larger than the external Auger rate. Another important process during the cascade is nuclear capture. This occurs predominantly from s and p states, and is important even for states of nominally large n and l because strong electric fields (10^8–10^9 V/cm) occurring during

